JOURNAL OF AIRCRAFT
Vol. 38, No. 2, March–April 2001

Near-Wake Measurements of a Delta Wing in a Supersonic Stream

Ivana M. Milanovic* and Iraj M. Kalkhoran†
Polytechnic University, Brooklyn, New York 11201

The near-wake region of a 75-deg sweptback delta wing was studied experimentally in a Mach 2.49 stream. Five-hole conical probe measurements were conducted vertically and horizontally through the primary vortices at the trailing edge and half-chord downstream of the planform for 7- and 12-deg angles of attack. The Mach number and pressure distribution profiles are summarized, and comparisons of flow properties at different survey stations are presented. A novel calibration approach using a three-dimensional Navier–Stokes solver to generate numerically the calibration data for a blunt-nosed five-hole conical probe over a range of Mach numbers and pitch angles was employed. The magnitude of the pitot, total, and static pressure deficits in the wake region increased with increasing angle of attack for the same measurement plane and decreased with the downstream distance. The swirl profiles have supersonic and high transonic peak magnitudes, and estimated core dimensions suggest vortex stretching in the vertical direction and convection downstream. A decrease in the radial Mach number component confirms the vortex trajectory changes from a strong downward flow over the planform to a gradual return toward the freestream in the near wake. Unlike the experimental results from transonic and low-speed leading-edge vortices, the axial and total Mach number distributions in supersonic vortices are found to be wakelike.

Nomenclature

c	=	chord length
D_N	=	five-hole conical probe flat nose diameter (Fig. 1)
M	=	Mach number
M_N	=	component of Mach number normal to the leading edge, $M_\infty \cdot \sqrt{(1 - \sin^2\alpha \cdot \cos^2\Lambda)}$
P	=	pressure
x, y, z	=	Cartesian coordinates
α	=	angle of attack
α_N	=	angle of attack normal to the leading edge, $\tan^{-1}(\tan\alpha/\cos\Lambda)$
Λ	=	wing leading-edge sweep angle
ν	=	uncertainty
χ	=	pressure tap distance from probe tip measured along the probe axis (Fig. 1)

Subscripts

a, b, c, d, e	=	conical probe pressure tap labels (Fig. 1)
x, y, z	=	Cartesian coordinates
01	=	condition ahead of the shock
02	=	condition behind the shock
0∞	=	settling chamber
∞	=	freestream

Introduction

EXTENSIVE theoretical and experimental research has indicated that vortical flows can have either benign or baleful consequences in the operational characteristics of aerospace vehicles, depending on the particular circumstances. However, the extent to which the benefits or drawbacks of vortical flows can be assessed rests on a thorough understanding of their behavior. The renewed interest in sustained supersonic flight, both civilian and military, created a need for information on the vortex wakes of aerodynamic components to access issues such as environmental impact, missile aft control surface effectiveness, and mixing. As one specific example, vortices determine the initial dispersion, mixing, and the ultimate residence time of ozone depleting species from engine exhaust in the stratosphere for supersonic transport (SST) aircraft. The inability to assess properly the environmental impact of a large SST fleet eventually contributed to its demise in the United States in the 1970s. In the two and a half decades that followed, significant progress was made in the photochemistry of ozone layers. However, the advances in understanding characteristics of leading-edge vortices in supersonic flows remained stagnant. The need for research on the dynamics of supersonic vortices to support the overall aim of a commercially viable SST fleet was again reiterated in two recent international meetings.[1,2]

Because of their aerodynamic attributes, delta wings are routinely incorporated in the design of supersonic vehicles. Surprisingly, although investigations of delta wing flowfields in supersonic streams date back to the 1950s, measurements in their vortices remain extremely scarce at best. This state of affairs is likely due to the challenging nature of obtaining reliable data in supersonic streams, particularly in shock- and vortex-dominated flowfields. Consequently, details of supersonic leading-edge vortices remain unknown, the lack of which has prevented understanding of these flowfields and validation of computational solutions. Vortex-wake flows of the delta planform with a subsonic leading edge in a supersonic stream were envisioned to be similar to their low-speed counterparts.[3,4] Some experimental information on the wake of low-speed delta wings has been provided by Hummel,[5] Hiremath et al.,[6] and Miller and Williamson[7] and may be helpful in understanding and identifying various flow mechanisms in the supersonic case. Immediately after leaving the planform, leading-edge vortices in the near wake move slightly downward and start to turn toward the freestream path.[6] A small reduction in the vortex strength can be explained by the termination of continuous vorticity influx from the wing surface. On the other hand, the trailing-edge vortex sheet has been found to interact with the leading-edge vortices.[5] This interaction produces an augmentation in the strength of the combined vortex system because the trailing-edge vortices do not simply dissipate. Also present in the near field, the secondary vortex decays rapidly downstream of the trailing edge.

Received 4 July 1999; revision received 8 November 2000; accepted for publication 1 December 2000.

*Graduate Teaching Fellow, Department of Mechanical, Aerospace, and Manufacturing Engineering; currently Assistant Professor, Department of Mechanical Engineering Technology, University of Hartford, West Hartford, CT 06117-1599. Member AIAA.

†Associate Professor, Department of Mechanical, Aerospace, and Manufacturing Engineering. Senior Member AIAA.

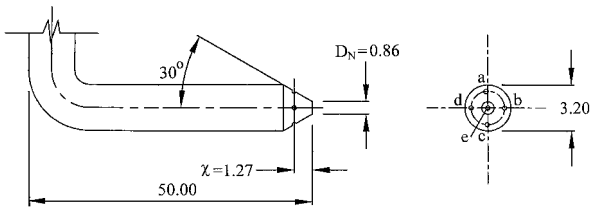

Fig. 1 Five-hole probe.

The first measurements in the wake of a supersonic delta wing appear to be in a series of NACA/NASA studies as represented by Perkins and Canning,[8] Boatright,[9] and Centolanzi.[10] In these early works, downwash, sidewash, pitot, and occasionally Mach number measurements with coarse spatial resolutions were made to evaluate the accuracy of several theoretical vortex-wake models. The pitot pressure data of Ref. 8 indicated wake characteristics similar to those in subsonic flow. Specifically, with increasing incidence angles the viscous wake displaced downward, it expanded slowly, and its intensity was reduced. In addition, a maximum pressure deficit location deflected downward for inboard spanwise locations and upward for the outboard locations. Regions of low dynamic pressure were found to exist at various spanwise locations, presumably due to the presence of concentrated vorticity. These results suggested that the wake is better interpreted as a region of vorticity instead of a vortex sheet.[9]

Optical techniques such as laser Doppler velocimetry (LDV) and partical image velocimetry (PIV), when applied to vortical flows at supersonic Mach numbers, suffer from the inability to maintain seeding in the core regions.[11,12] Those seeding particles that remain in the cores do not realistically follow the flow. Furthermore, as illustrated in the work of Ganzer and Szodruch,[13] each surveyed location requires multiple and separate measurements with extensive data manipulation. Information obtained from these techniques is, therefore, uncertain and misleading at times. Moreover, LDV and PIV measurements, if successfully carried out, cannot provide the pressure and Mach number information, which are of great interest in characterizing compressible flows, without introducing additional assumptions.

In the light of the aforementioned, a five-hole cone probe of 30-deg half-angle (Fig. 1) was found to be the most suitable diagnostic tool for the current supersonic vortex-wake measurements. The principle of a multihole conical probe is based on the notion that Mach number, pressure, and directionality of the incoming stream may be correlated with the combination of pressure readings on the conical probe surface and the pitot port situated at the flat tip. To circumvent the traditional experimental calibration vastly demanding on resources, an alternative numerical calibration procedure was employed in the recent work of Milanovic and Kalkhoran.[14] The probe responses under various conditions were simulated with a three-dimensional thin-layer Navier–Stokes solver (TLNS3D) of Vatsa and Wedan.[15] The TLNS3D code was a logical choice for the flow simulation around a flat-nosed cone probe because it was developed and validated to solve external aerodynamic problems, including those of axisymmetric blunt bodies at high speeds. The validity of the computed pressure distributions on the probe surface was subsequently confirmed in a series of wind-tunnel tests including low Mach number and high-angularity flowfield. Thus, the numerical approach was shown to enhance the calibration data acquisition in manners that are conductive economically without suffering from the lack of desired accuracy.

With a three-dimensional thin-layer Navier–Stokes solver, the calibration data were generated for the range of Mach numbers and pitch angles of interest. It is evident that experimental data on delta wing vortex-wake at supersonic speeds are quite rare. Their physics are highly complex because various vortex systems interact continuously with one another while being convected downstream. Current understanding of this flowfield is largely based on flow visualization data, from techniques such as light sheet/vapor screen, shadow, and schlieren photographs. Although topological similarities between low- and high-speed flows exist, the quantitative details remain largely unknown. To advance understanding of vortices in supersonic flows and contribute to the limited available database, the present authors initiated an experimental study of the vortices from a 75-deg sweptback delta wing in a Mach 2.49 stream at 7- and 12-deg angles of attack. Of particular interest were Mach number and pressure distributions in the leading-edge vortices. Five-hole probe surveys were first conducted vertically and horizontally through the primary vortices at the trailing-edge plane. With the initial conditions of the vortex wake characterized, the study continued into the near wake. Primary vortices were then surveyed at 0.5 chord length downstream of the trailing edge for the same incidence angles. The present paper summarizes the findings of these near-wake surveys and presents comparisons of flow properties at different survey stations.

Facility and Experimental Setup

The delta wing near-wake investigation was conducted in Polytechnic University's supersonic wind tunnel. It is a blowdown facility exhausting to the atmosphere[16] with a square test section measuring 0.381 × 0.381 and 1.2 m in length. Experiments were carried out in a Mach 2.49 stream with the nominal stagnation temperature and pressure of 290 K and 0.35 MPa, respectively. The Reynolds number based on the root chord of the wing model is, thus, 3.5×10^7. The duration of a typical wind-tunnel run was 3 s, with data acquisition during the final 2 s. This is considered sufficient because bench-top tests for the employed probe have revealed a response time of approximately 0.5 (Ref. 17).

A generic representation of the experimental arrangement is shown in Fig. 2. The model planform is a 75-deg sweptback, flat-top delta wing with leading and trailing edges chamfered at 30 deg. It has a 152.4-mm root chord, a thickness-to-root chord ratio of 0.04, and an aspect ratio of 1.07. The delta wing model is welded to a streamlined strut with a double-wedge airfoil section. The strut connects the lower surface of the wing to a two-degree-of-freedom traversing mechanism on the test section floor. This arrangement allows movement of the wing model in the longitudinal and horizontal direction so that continuous measurements in the cross plane can be made. Vortices of different strength are generated by placing the delta planform at various angles of attack. The present study utilized two moderate incidence angles of 7 and 12 deg.

When advantage is taken of the flow symmetry over the wing, which was confirmed by surface oil vizualizations,[14] five-hole conical probe surveys were carried out on the port side only. Measurements were taken at two axial stations, namely, at the trailing edge

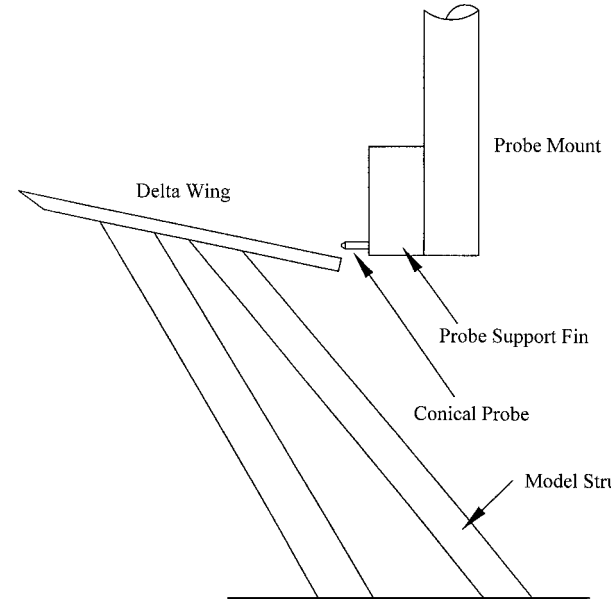

Fig. 2 Schematic of experimental arrangement.

and 0.5 chord downstream of the trailing edge. The probe was fitted inside of a 25-mm-diam stainless steel tube to provide structural integrity. A wedge-shaped fin with an 18-deg included angle was installed with its leading edge 13 mm behind the probe tip to isolate the conical probe from any upstream influence. The entire assembly could traverse vertically, thus permitting surveys at different heights relative to the wing. The pressure lines connected to the five orifices on the probe were fed through the support tube to pressure transducers located outside of the wind tunnel.

Shadowgraph flow visualizations were performed with an air-spark light source providing microsecond range exposure times. Surface and pitot pressure readings on the five-hole probe were measured with Kulite™ pressure transducers (models ITQ-1000-10-A and ITQ-1000-50-A). A Validyne™ AP10-50-A absolute pressure transducer was used to obtain the tunnel settling chamber pressure. The output signals were converted, amplified, and recorded with a LeCroy™ 6810 Waveform Digitizing/Recording system at 4880 Hz. The total uncertainty levels associated with the primary measurements of cone surface, pitot, and chamber pressure, which account for nonlinearity, hysteresis, and repeatability of the transducers, were $\nu_c = \pm 0.345$, $\nu_{02} = \pm 1.73$, and $\nu_{0\infty} = \pm 4.31$ kPa, respectively.

Experimental Results and Discussion

Vertical Surveys

For the present wing model at incidence angles of 7 and 12-deg, the corresponding normal angles of attack are $\alpha_N = 25.4$ and 39.4-deg. In the Mach 2.49 stream, both cases have a subsonic leading edge with respective normal Mach numbers of $M_N = 0.71$ and 0.82, generating primary vortices by separated flow along the leading edge. Spark shadowgraphy was first used to obtain a global assessment of the vortex positions. In such an integrated view, due to lower density levels than that of the freestream, vortex cores are manifested as dark conical regions surrounded by a brighter periphery, convecting downward from the apex of the wing. Representative shadowgraphs illustrating both the leeward and the near wake are shown in Figs. 3 and 4, where flow is from left to right. In Figs. 3 and 4, the dark vortex core and the white bands associated with its boundaries are clearly seen approximately up to 0.25 chord behind the trailing-edge. After leaving the planform, the vortex passes through the trailing-edge shock waves and bends upward. In the portion from 0.25 to 0.5 chord behind the wing, the lower vortex trail is still entirely visible, unlike the upper boundary. The upper trail appears to interact with the shock wave and subsequently coincide with it. Also seen is the trailing-edge wake, just below the vortex core, with its lower boundary being the other white band. Shadowgraphs taken with the five-hole conical probe installed indicated that no vortex breakdown, either natural or probe induced, had occurred.

Flow visualizations suggested a larger size and higher elevation of the vortex core above the wing with increasing angle of attack, which was also confirmed by the subsequent conical probe

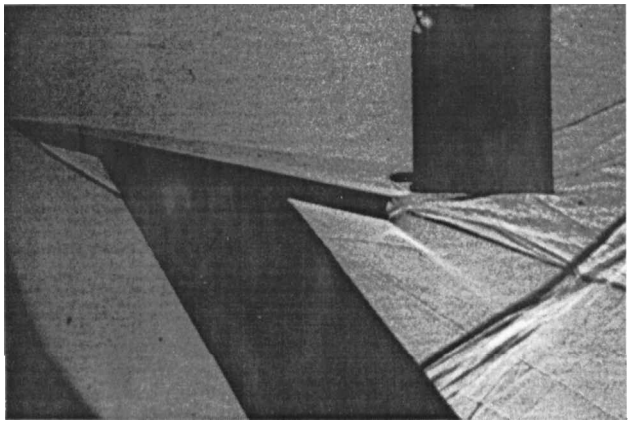

Fig. 3 Shadowgraph of typical five-hole probe survey at $z/c = 0$ plane ($\alpha = 12$ deg and $M_\infty = 2.49$).

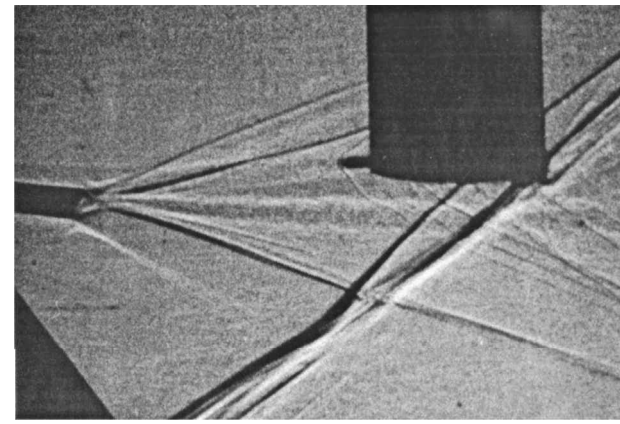

Fig. 4 Shadowgraph of typical five-hole probe survey at the $z/c = 0.5$ plane ($\alpha = 7$ deg and $M_\infty = 2.49$).

measurements.[14] When the development is followed of the white regions outlining the general vortex core boundaries, the shadowgraphs of the near wake depict the apparent change of the trajectory followed by a vortex core enlargement. At the trailing edge, both expansion and shock waves can be seen. Behind the trailing edge, a recompression shock, laying just below the vortex, is also apparent. The viscous wake from the wing trailing edge is seen to have a gradual downward trajectory, which is due to the downwash created by the leading-edge vortices. The presence of nearby waves and auxiliary vortical structures is expected to influence pressure and Mach number profiles of the primary vortices in the near field.

Shadowgraphs for each incidence angle were also utilized to establish the general vicinity of the vortex core in the vertical direction. Additional horizontal and vertical traverses of the five-hole probe were made to verify the exact location of the minimum pitot pressure, which was utilized as a reference point. Vertical and horizontal surveys were then conducted through the primary vortices at the trailing edge and 0.5 chord downstream. The results are presented in a Cartesian coordinate system. With the origin situated at the intersection of the leading and trailing edges x is along the span, and y and z represent the directions perpendicular and parallel to the freestream.

For the 7-deg vortex, the normalized pitot pressure at the trailing edge plane has a minimum of 0.121, located at $x = 16$ and $y = 5.5$ mm. At $\alpha = 12$ deg, the minimum $P_{02}/P_{0\infty}$ ratio was found to be at $x = 22$ and $y = 8.4$ mm, with a value of 0.07. The probe was then traversed vertically through the aforementioned locations in increments ranging from 0.5 to 2 mm. These surveys covered the upper portion of the vortices and the region immediately below the core centers because the data collection was restricted by the presence of the wing surface. At a half-chord downstream of the planform, the reference normalized pitot pressure value for 7-deg case was 0.149, located at $x = 15$ and $y = 3.3$ mm. In the 12-deg vortex, a minimum pitot pressure of 0.094 was found at $x = 19.5$ and $y = 4.6$ mm. Vertical surveys at $z/c = 0.5$ plane were performed with a constant spatial resolution of 1 mm. The pitot pressure distributions at both measurement stations are presented in Figs. 5 and 6.

During vortex evolution over the wing, a continuous influx of vorticity from the leading edge is feeding into the core. This process terminates at the trailing edge, and vortices shedding into the wake would experience an immediate reduction in their strength.[5] As a result, the minimum pitot pressure values at a half-chord station downstream of the wing are higher than those at the trailing-edge plane. Because the measurements were made in the near field, the vortex strength reduction as indicated by pitot pressure is not drastic. As vortices convect downstream, a descending trajectory is noticed. The minimum pitot pressure locations at half chord, when compared to those at the trailing edge, are shifted downward for both incidence angles. The downward motion of the vortex wake results from the mutual induction of primary vortices, a common feature illustrated in both low[5,6] and high-speed[8,9] flows. At both surveyed

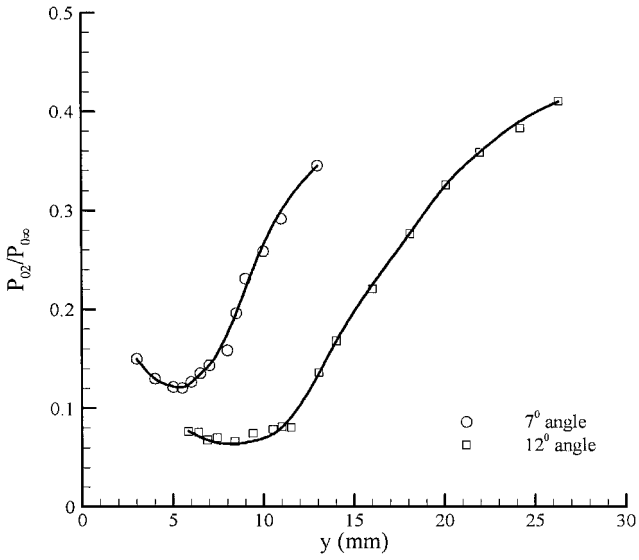

Fig. 5 Pitot pressure distribution from the vertical surveys at $z/c = 0$.

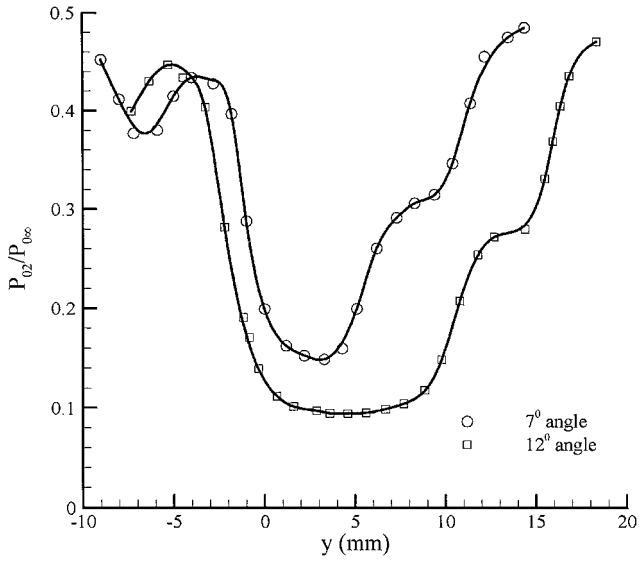

Fig. 6 Pitot pressure distribution from the vertical surveys at $z/c = 0.5$.

stations, a higher incidence angle is accompanied by a larger pitot pressure deficit. In addition, the 12-deg case exhibits an almost flat pressure distribution around the minimum value. The extent of this constant pressure region increases from 5 mm at the trailing edge to 7 mm at the downstream measurement plane. This results in bucketlike pitot pressure profiles as opposed to a cusp-shape distribution characteristic for the lower angle of attack vortex.

The pitot pressure change in the upper part of the vortex core at the downstream survey station shown in Fig. 6 does not exhibit a smooth transition into the freestream value. This may be attributed to the numerous waves emanating from the trailing edge as seen in the shadowgraphs. Additional disturbances are also anticipated from the change of the vortical trajectory, initially downward and oblique over the wing and then turning toward the freestream as vortices trail off the planform. Furthermore, the lower portion of the core has steeper gradients, presumably influenced by the wake flow from the trailing edge. Shadowgraphs indicate the trailing-edge wake immediately below the leading-edge vortices, and this is further substantiated by an additional pitot pressure deficit area just below that of the primary vortex.

The measured total and static pressures are presented in Figs. 7–10. As expected, significant deficits in these quantities are present in the core regions at both measurement planes. Figure 7 shows the total pressure distribution in the primary vortices at the

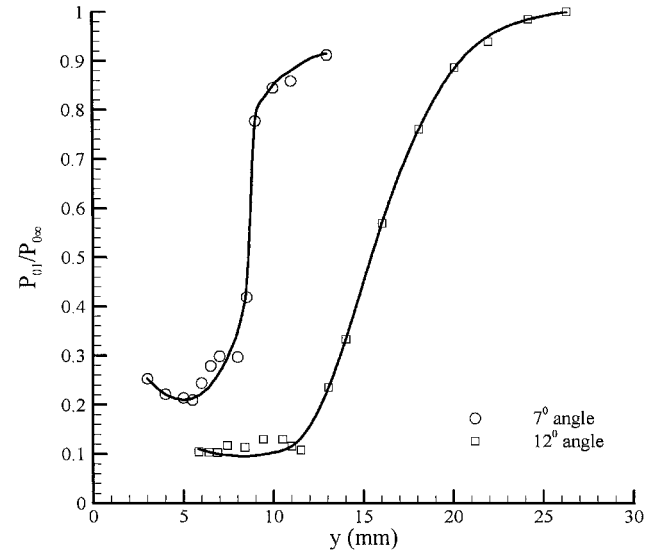

Fig. 7 Total pressure distribution from the vertical surveys at $z/c = 0$.

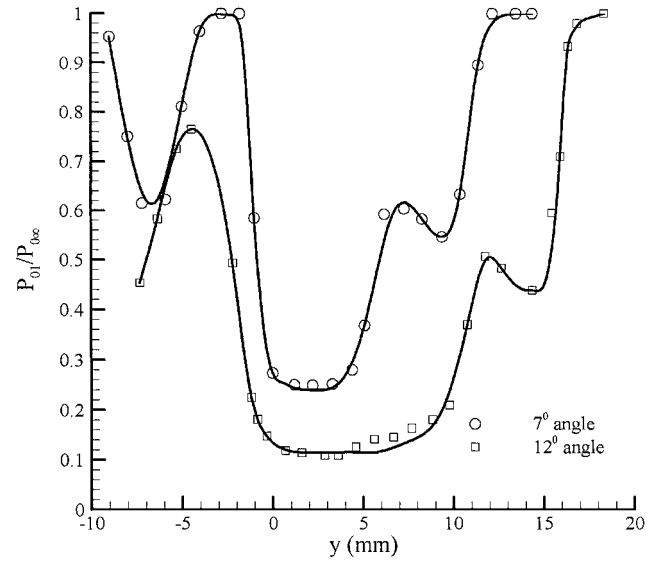

Fig. 8 Total pressure distribution from the vertical surveys at $z/c = 0.5$.

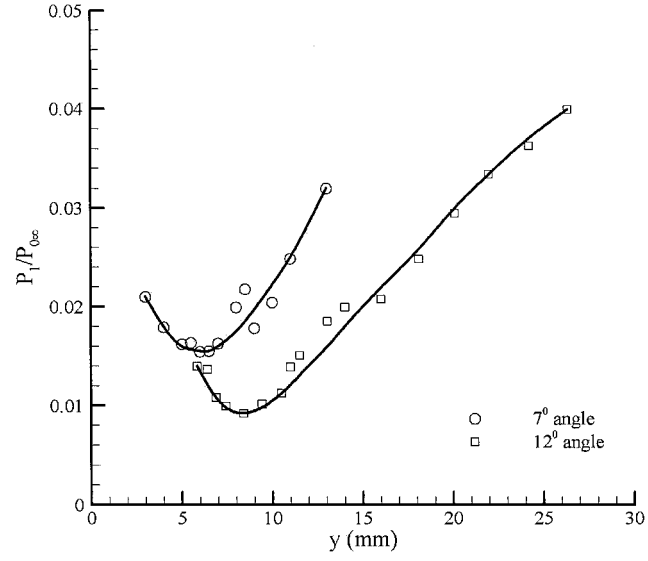

Fig. 9 Static pressure distribution from the vertical surveys at $z/c = 0$.

Table 1 Minimum pressures in the leading-edge vortices

	Trailing-edge measurement plane, $z/c = 0$		Near-wake measurement plane, $z/c = 0.5$	
	$\alpha = 7^\circ$	$\alpha = 12^\circ$	$\alpha = 7^\circ$	$\alpha = 12^\circ$
$(P_{02}/P_{0\infty})_{\min}$	0.1210	0.0700	0.1490	0.0940
$(P_{01}/P_{0\infty})_{\min}$	0.2100	0.1000	0.2520	0.1260
$(P_1/P_{0\infty})_{\min}$	0.0154	0.0092	0.0210	0.0170

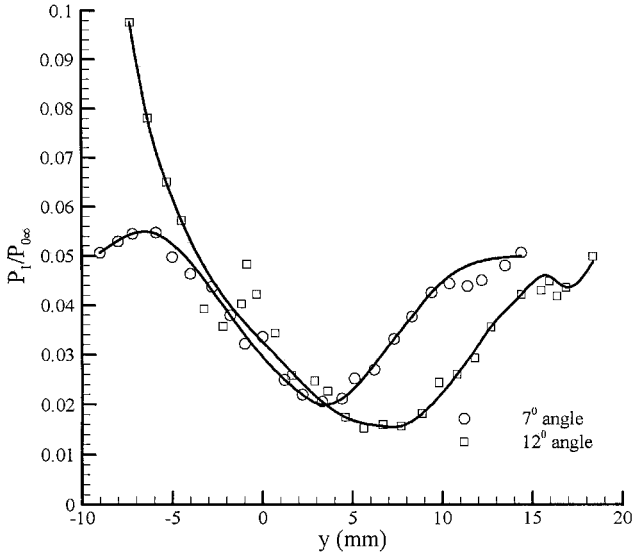

Fig. 10 Static pressure distribution from the vertical surveys at z/c = 0.5.

trailing edge. The minimum values for the 12- and 7-deg vortices are $P_{01}/P_{0\infty} = 0.1$ and 0.21, respectively. Their counterparts at $z/c = 0.5$ station given in Fig. 8 are 0.126 and 0.252. Similar to the pitot pressure results, the higher angle-of-attack case is accompanied by a flat total pressure region growing in size with the downstream distance. Meanwhile, the lower incidence angle has cusp-shaped pressure profiles at both surveyed stations. The pressure profiles behind the wing also exhibit asymmetries, which can be attributed to the presence of the trailing-edge wake and waves emanating from the planform. Figure 9 illustrates the static pressure profiles at the trailing edge. The normalized static pressure drops well bellow its freestream value, reaching a minimum of $P_1/P_{0\infty} = 0.0092$ and 0.0154 for the 12- and 7-deg cases, respectively. The corresponding values half a chord downstream are 0.017 and 0.021 as seen in Fig. 10. Overall, the magnitudes of the pitot, total, and static pressure deficits increase with increasing angle of attack at the same measurement plane and decrease with the downstream distance from the model. Table 1 summarizes minimum pressure values in the primary vortices of the present delta wing at the two surveyed locations.

The swirling pattern is revealed by the Mach number component perpendicular to the direction of the survey. Therefore, M_x distributions in the current vertical surveys delineate the swirl character. The M_x profiles for both incidence angles in the near wake are shown in Figs. 11 and 12. The swirl in the vertical surveys resembles the tangential velocity profile of the classical low-speed Lamb–Oseen vortex with a linear distribution in the viscous core and decay with increasing distance from the core. As seen in Fig. 11, swirl Mach numbers at the trailing edge reach a maximum of 1.07 and 1.14 for the 7- and 12-deg cases, respectively. These low supersonic values are expected as the flow with an already transonic normal Mach number accelerates around the sharp leading edge.

The swirl profiles at the wake station $z/c = 0.5$ are summarized in Fig. 12. The peak M_x values found at the upper and lower edges of the core for the 7-deg incidence angle are 0.8 and −0.98. Corresponding magnitudes for the 12-deg angle of attack are 0.91 and −0.96. A slightly larger swirl at the lower portion of the vortices is present in both cases. The core dimensions, as indicated by the distance between the two local peak values in swirl profile, are 7.2 and 13 mm for the 7- and 12-deg vortices, respectively. A comparison of the core size between two measurement planes is complicated by the restrictions in obtaining data near the planform surface. However, estimated[14] vertical dimensions for the 7- and 12-deg vortices at the trailing edge are 5.6 and 10.8 mm, respectively. These measurements, thus, suggest stretching of the vortex core in the vertical direction and convection downstream. Primary vortices at the trailing edge, bound by the wing surface beneath, develop into an elliptical shape with the horizontal axis as the major axis. Downstream of the trailing edge, the vortices are no longer restricted by the planform and the core would start to adjust its shape. Suppressed over the wing, the vortex vertical axis becomes the dominant one in the near wake, as illustrated in the laser vapor sheets of Ganzer and Szodruch.[13] In the far wake, vortices would eventually reach more axisymmetric profiles. The downstream distance needed for this would likely depend on the incidence angle and the influence of various flow parameters.

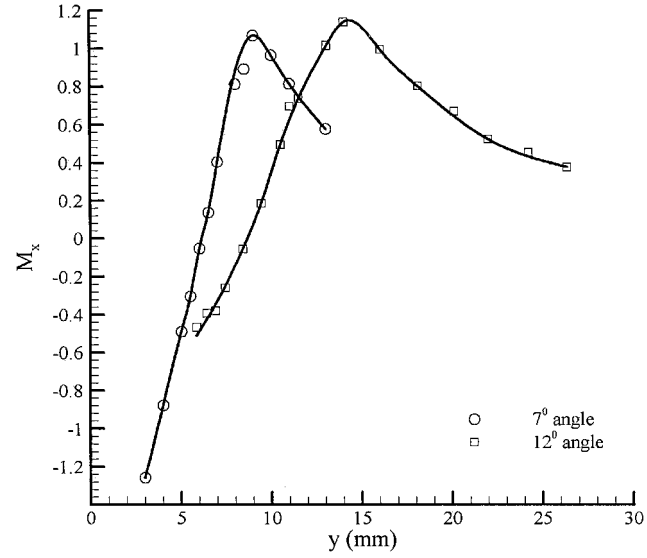

Fig. 11 Swirl Mach number from the vertical surveys at z/c = 0.

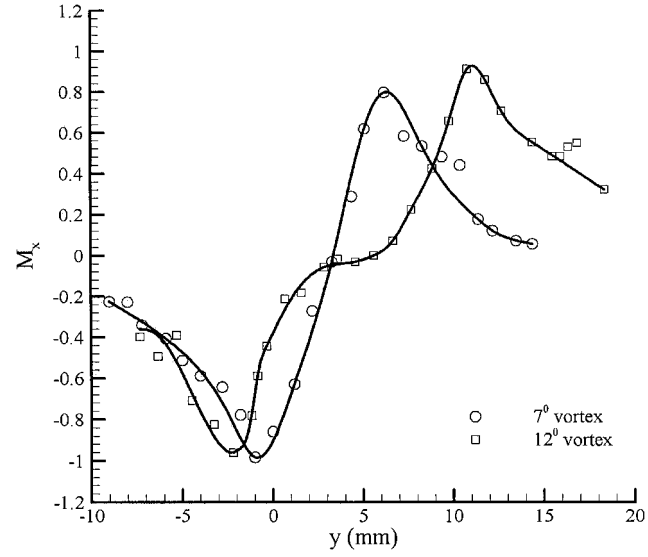

Fig. 12 Swirl Mach number from the vertical surveys at z/c = 0.5.

Figures 13 and 14 illustrate the radial Mach number M_y distributions. The magnitude of M_y is determined by the radial growth of the vortex structure and mutual induction of the vortex pair. The M_y profiles at the trailing-edge plane presented in Fig. 13 exhibit peaks in the high transonic and sonic regions, indicating a substantial downward flow. The maximum values obtained for the 7- and 12-deg

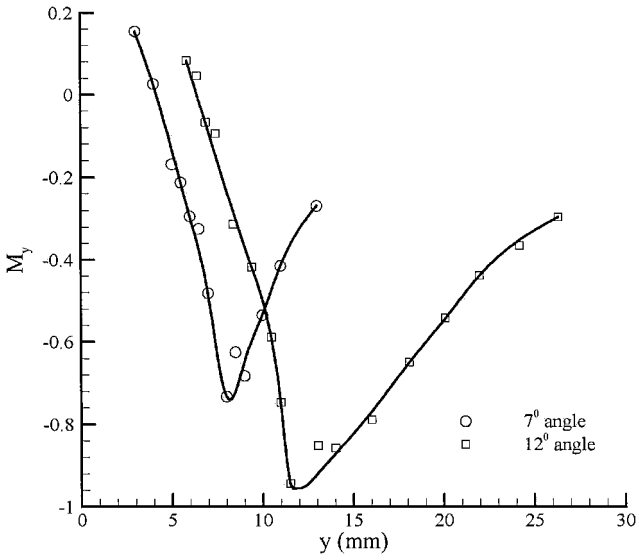

Fig. 13 Radial Mach number from the vertical surveys at $z/c = 0$.

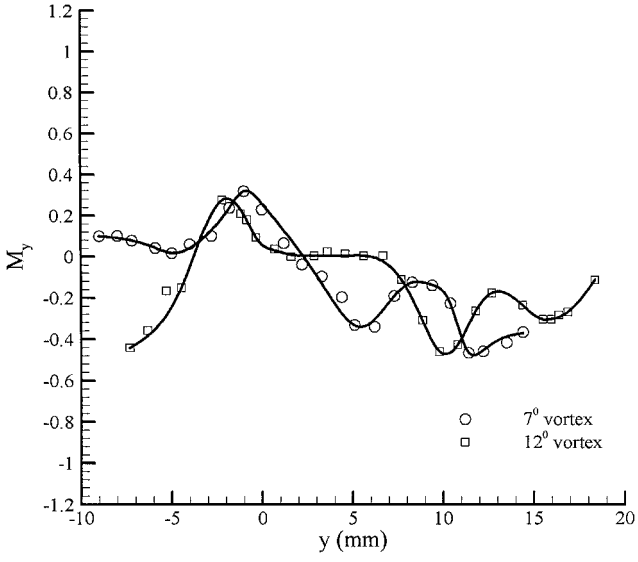

Fig. 14 Radial Mach number from the vertical surveys at $z/c = 0.5$.

vortices are −0.73 and −0.94, respectively. The *My* distributions at the $z/c = 0.5$ station shown in Fig. 14 have nevertheless reduced significant peaks with locations closely corresponding to the upper and lower core boundaries. Maximum radial magnitudes above and below the vortex center for 7-deg incidence angle are −0.34 and 0.32, respectively. In the case of a 12-deg angle of attack, these values are −0.46 and 0.28. A decrease in the downward component of the flow again confirms the vortex trajectory changing from an obliquely downward flow over the planform to a gradual return toward the freestream direction in the near wake. Mach number gradients in the proximity of the core center differ considerably for the two angles in the wake station. The 12-deg vortex is characterized by an approximately 6-mm-wide region of low radial values closely corresponding to the vortex center, whereas the 7-deg case has a nearly linear change of M_y within the core. A large inward component found immediately above the wing suggests boundary-layer entrainment into the core. Also note that entrainment characteristics of the vortices at the trailing edge continue into the near wake. At the core edges, large M_y components are directed toward the vortex center. Such a feature would be important in assessment of the stratosphere ozone depletion issue because exhaust products entrained in the descending vortex pair would give rise to a very different resident time of the exhaust species.

The distributions of axial, M_z, and total Mach numbers M are presented in Figs. 15–18. At each survey station, M_z and M exhibit

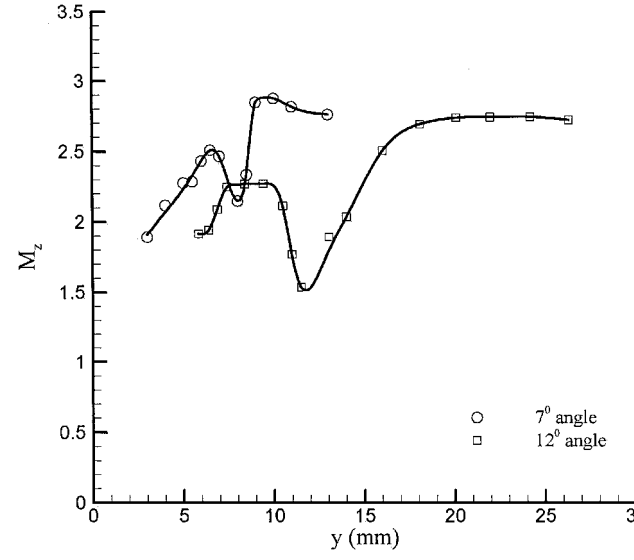

Fig. 15 Axial Mach number from the vertical surveys at $z/c = 0$.

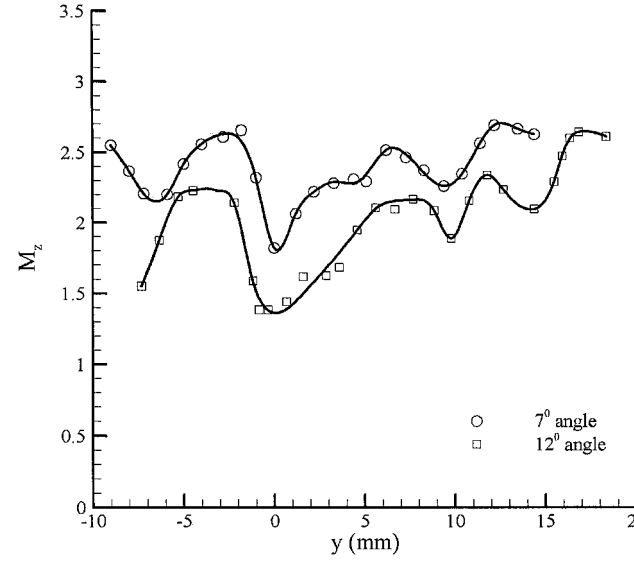

Fig. 16 Axial Mach number from the vertical surveys at $z/c = 0.5$.

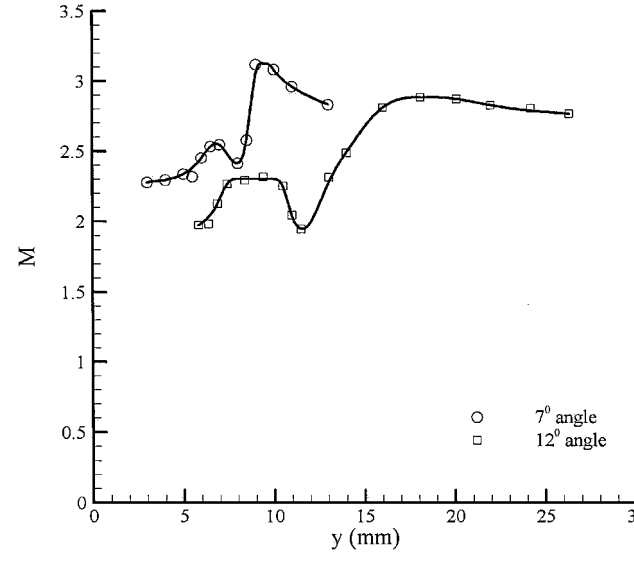

Fig. 17 Total Mach number from the vertical surveys at $z/c = 0$.

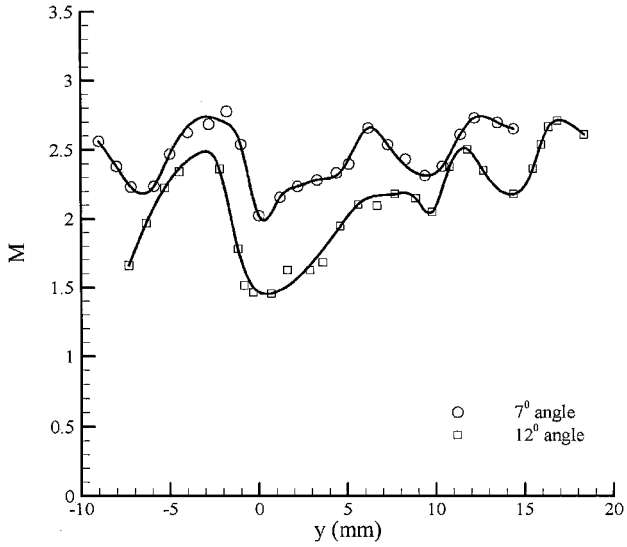

Fig. 18 Total Mach number from the vertical surveys at $z/c = 0.5$.

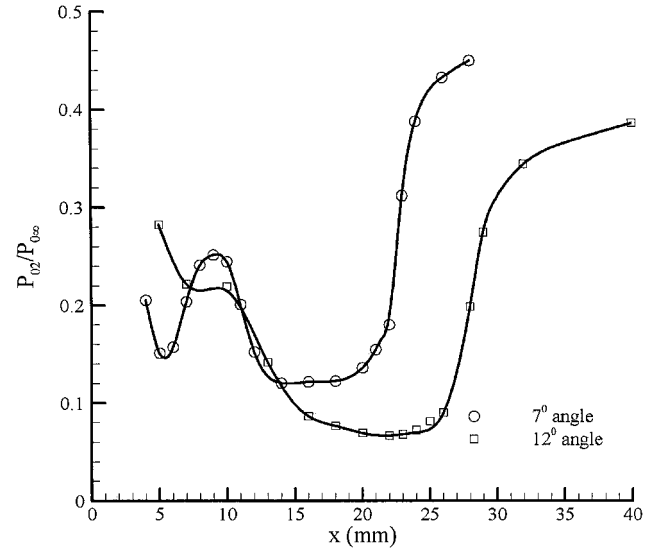

Fig. 19 Pitot pressure distribution from the horizontal surveys at $z/c = 0$.

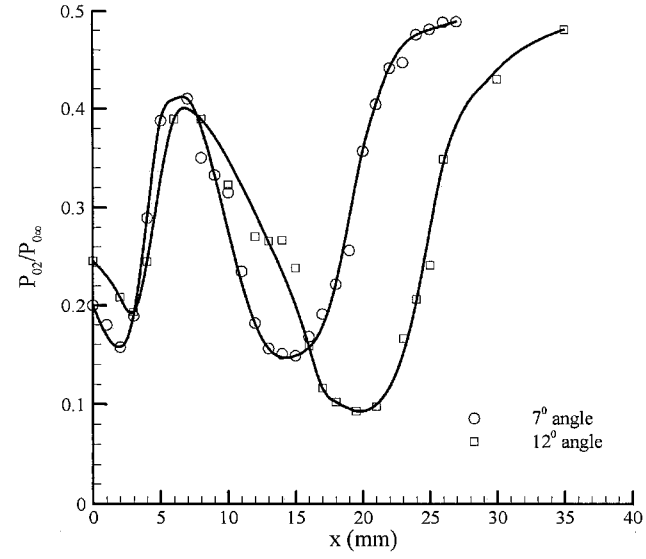

Fig. 20 Pitot pressure distribution from the horizontal surveys at $z/c = 0.5$.

similar trends, illustrating the dominant contribution of the streamwise component on the overall Mach number. The vortex cores were found to have wakelike Mach number profiles at both measurement planes. At the trailing edge, the minimum axial Mach number in the core region of the 7-deg vortex is 2.15, as seen in Fig. 15, and the matching total Mach number 2.41 is shown in Fig. 17. The corresponding values for the 12-deg case are $M_z = 1.53$ and $M = 1.95$. Considerable differences in magnitudes between axial and total Mach numbers stem from the large downward component of the flow. The Mach number overshoot above the core is caused by two mechanisms. First, the planform at an angle of attack creates an expanded flow on the leeward side that surrounds the vortices. In addition, the crossflow is being accelerated due to the expansion around the leading edge. On the other hand, as a result of entraining boundary-layer fluid into the vortex, Mach numbers at the lower portion of the core do not reach a value higher than that of the freestream.

At the wake measurement plane $z/c = 0.5$, the axial Mach number in the core center of the 7-deg vortex is 2.276, as seen in Fig. 16, and the matching total Mach number of 2.28 is shown in Fig. 18. The corresponding values for the 12-deg case are $M_z = 1.94$ and $M = 1.95$. The larger spatial extent of the Mach number deficit region behind the trailing edge is believed to be due to the expansion of the core in the vertical direction during the downstream convection because the vortex is no longer restricted by the presence of the wing surface. It is also expected that the magnitude of the Mach number deficit in the core is reduced as the vortex convects and relaxes further into the far wake. The rate at which this process occurs is, however, complicated by a number of phenomena present in the near wake. As stated before, the trailing-edge viscous wake is immediately below the vortex. Behind the wing, this low Mach number structure is merged with the lower portion of the vortex. Inferred from the radial Mach number profile at the half-chord station presented in Fig. 14, the leading-edge vortex in the wake is able to entrain the surrounding flow. Consequently, low-momentum fluid from the trailing-edge wake would be entrained into the primary vortices, further contributing to the Mach number deficit in the cores. In addition, compression waves from the planform trailing edge interact with the vortices upstream of the $z/c = 0.5$ location. This would also foster a slower relaxation of the Mach number deficit in the cores. Secondary vortical structures and waves generated by the vortex trajectory, changing from the leeward side to the near wake, would further complicate the character of the vortices. Consequently, M_z and M profiles at a half-chord away are not monotonically approaching the freestream value.

Horizontal Surveys

Measurements were also performed through the cores of primary vortices in the spanwise direction. At the trailing-edge location, these horizontal surveys were made 5.5 and 8.4 mm above the wing surface for 7- and 12-deg vortices, respectively. Corresponding heights at $z/c = 0.5$ station are $y = 3.3$ and 4.6 mm. The minimum spatial resolution employed during the survey was 1 mm. Pitot pressure distributions are shown in Figs. 19 and 20. Trailing-edge profiles illustrated in Fig. 19 reveal an asymmetric shape due to different flow structures present in the vicinity of the leading-edge and midspan locations. In the 7-deg case, an almost flat pitot pressure region covering 4 mm, or, equivalently, 0.1 of the local semispan, with an average value of $P_{02}/P_{0\infty} = 0.121$, was found. In addition to this minimum pitot pressure zone associated with the primary vortex, another well-defined pressure deficit was noted farther toward the leading edge. The latter is believed to result from the traverse in the vicinity of a secondary vortex core and through a vortex embedded in the shear layer. Surface oil flow visualizations[14] located the secondary vortex core within the limits of $x = 4$–9 mm, thus, it coincides with the pressure dip near the leading edge. The same region is also accompanied by wakelike axial/total Mach number profiles. Also, the vortex embedded in the shear layer at this angle of attack[18] is adjacent to the secondary vortex. However, a clear distinction between these two vortical structures is not possible without detailed mapping of the entire crossflow plane, which was beyond the scope of the current investigation.

As seen in Fig. 19, the normalized pitot pressure distribution in the viscous core for the 12-deg vortex exhibits a broader spatial scale with a lower minimum value of 0.07 compared to the 7-deg case. A distinctive second pitot pressure drop toward the leading edge was not found. This is attributed to the change in the incidence angle. When the angle of attack is increased, the primary vortex has a higher position relative to the wing, whereas the secondary vortex remains near the surface. The current 12-deg survey was carried out at a 0.21 semispan distance from the planform. This represents a value approximately twice that of predicted secondary vortex location.[19] Therefore, the secondary vortex is believed to be below the path of the horizontal traverse. In addition, a higher incidence angle would move the position of the shear-layer vortex further below the primary core.[18] In light of these considerations, it is likely that the influence of the secondary vortex and the shear-layer vortex has not been detected in the 12-deg horizontal traverse at the trailing edge.

Pitot pressure distributions in the downstream station shown in Fig. 20 again reveal two distinct deficits representing primary vortices and secondary vortical structures. Unlike pitot pressure profiles at the trailing edge (Fig. 19) characterized with wide and flat minimum pressure regions, primary vortices in the wake are exhibiting pronounced cusp pressure profile shapes. This change is again indicative of the vortex undergoing profound restructuring between the two surveyed locations. Also, a more significant pitot pressure recovery outside of the core in the direction of the leading edge is found, as compared to that of the $z/c = 0$ station. Greater outboard pitot pressure magnitudes are due to the spanwise relaxation process behind the model, providing for the displacement of the secondary vortex structure.

The total pressure distributions from the horizontal surveys are shown in Figs. 21 and 22. Similar to the pitot pressure profiles described earlier, the same two characteristic deficit regions were present in all investigated cases. Both primary vortices at the trailing-edge plane have an almost flat zone of minimum total pressure approximately 8 mm wide, as seen in Fig. 21. Plateau values of $P_{01}/P_{0\infty}$ for the 7- and 12-deg cases are 0.21 and 0.1, respectively. Pressure profiles in the leading-edge vortices at the $z/c = 0.5$ location illustrated in Fig. 22 are characterized by a smaller spanwise spatial scale as compared to their trailing-edge counterparts. Minimum total pressure regions at the wake station are covering about 3 mm each, with average values of 0.25 and 0.13 corresponding to lower and higher angle of attack. Consequently, an increase in an incidence angle is accompanied by a more pronounced total pressure deficit. The static pressure profiles are presented in Figs. 23 and 24. An almost constant minimum static pressure region 5 mm wide is found at the trailing-edge plane in both cases, as shown in

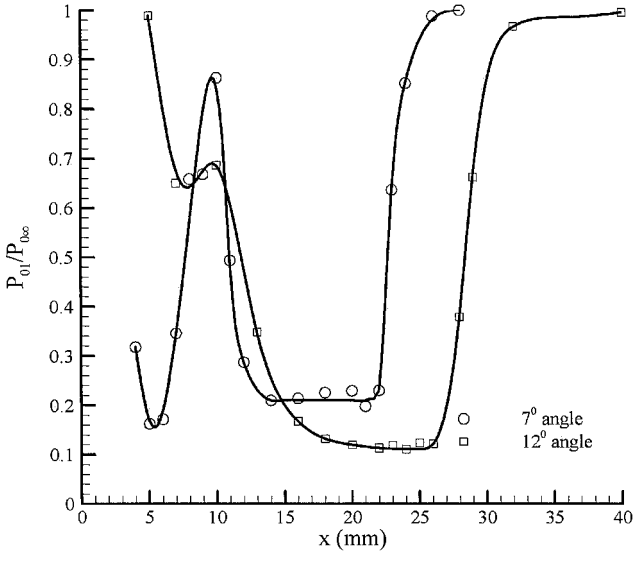

Fig. 21 Total pressure distribution from the horizontal surveys at *z/c* = 0.

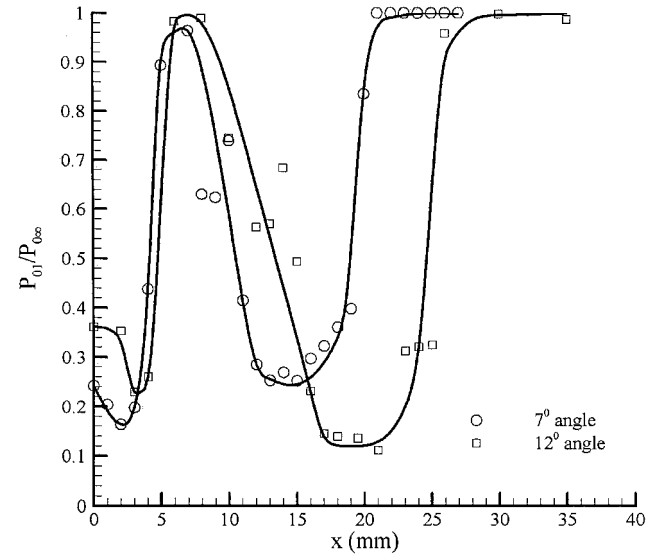

Fig. 22 Total pressure distribution from the horizontal surveys at *z/c* = 0.5.

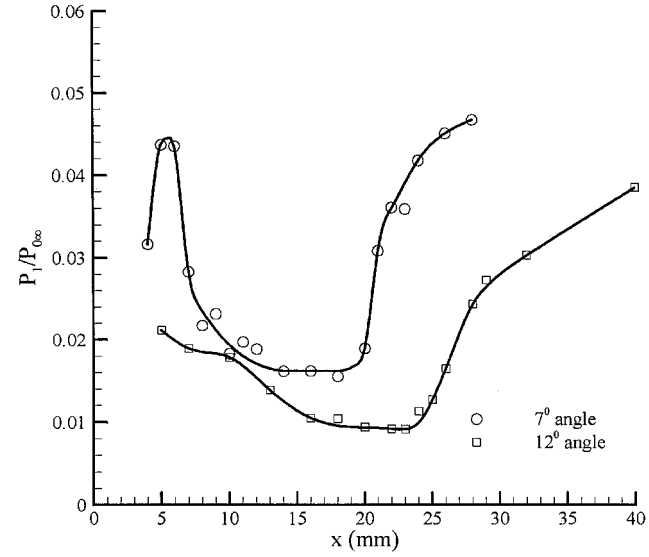

Fig. 23 Static pressure distribution from the horizontal surveys at *z/c* = 0.

Fig. 23. The associated average magnitudes are $P_1/P_{0\infty} = 0.0154$ and 0.0092 for the 7- and 12-deg vortices, respectively. Static pressure profiles in the wake summarized in Fig. 24 have distinct deficits, with earlier reported minimum values of 0.021 and 0.017 corresponding to lower and higher angle of attack.

Figure 25 presents the lateral Mach number M_x distribution at the trailing edge. Values of M_x at the midspan for both incidence angles are close to zero as expected. In traversing towards the leading edge, M_x has a general decreasing trend, which is an artifact of the conical nature of the flow over the planform. Near the leading edge, M_x distributions have a sharp rise to positive values, an indication of the shear layer generating strong flow toward the midspan. At the $z/c = 0.5$ measurement plane, after vortical trajectory adjustment, without the shear-layer feeding mechanism and the imposed restrictions from the wing surface, the M_x values at the core center are found to be close to zero as seen in Fig. 26. A notable feature is inward flow directed toward the center at the core edges, a characteristic also found in the vertical surveys. A continuous influx of the surrounding fluid into the core is, thus, expected as the vortex convects downstream.

The swirl Mach number M_y distributions at the trailing edge are summarized in Fig. 27. These profiles are the composite result of

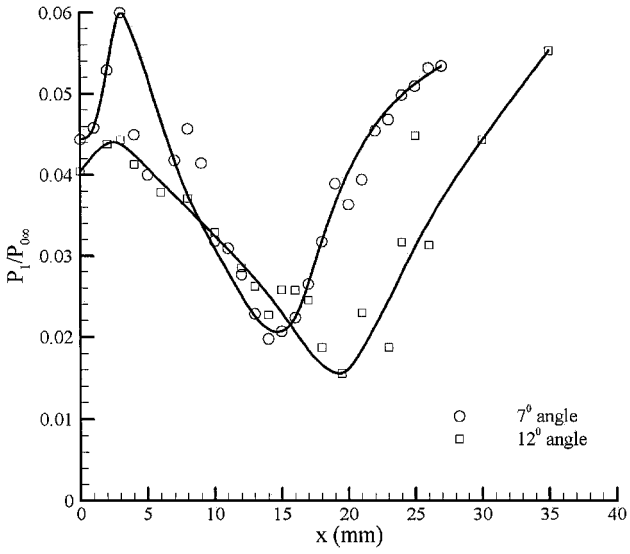

Fig. 24 Static pressure distribution from the horizontal surveys at $z/c = 0.5$.

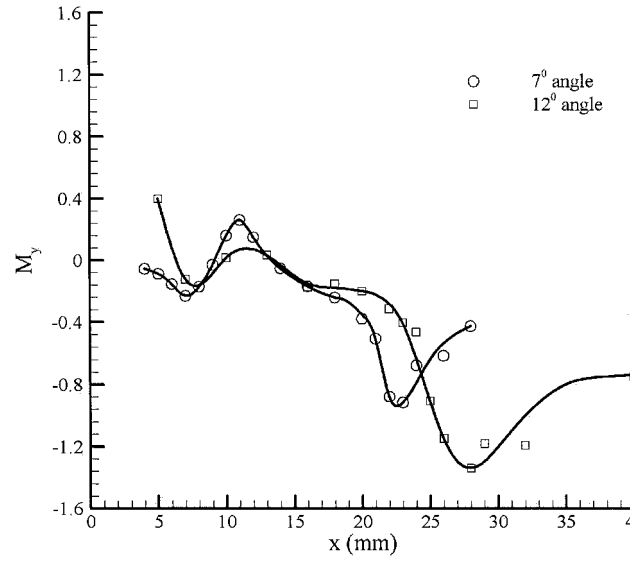

Fig. 27 Swirl Mach number from the horizontal surveys at $z/c = 0$.

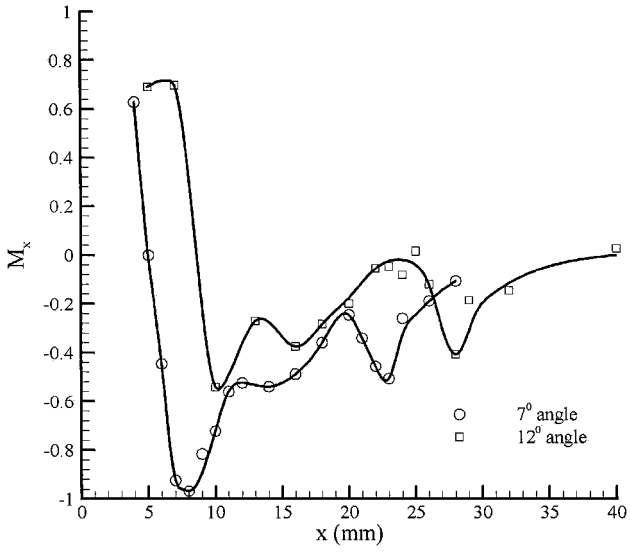

Fig. 25 Radial Mach number from the horizontal surveys at $z/c = 0$.

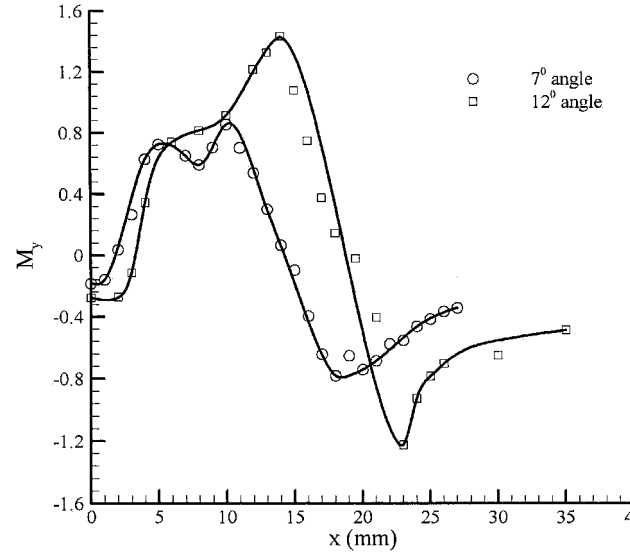

Fig. 28 Swirl Mach number from the horizontal surveys at $z/c = 0.5$.

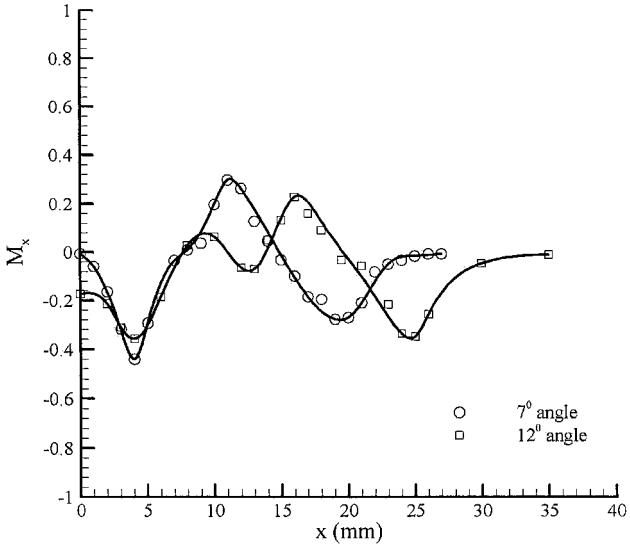

Fig. 26 Radial Mach number from the horizontal surveys at $z/c = 0.5$.

the downward convecting flow over the wing, shear-layer generation along the leading edge, secondary vortices, and the mutually induced flowfield by the primary vortices across the symmetry plane. Consequently, M_y has a substantial downward value in the midspan region, and its profile is without a distinctive second peak of an isolated vortex. The maximum M_y values are -0.92 and -1.34 for the 7- and 12-deg cases, respectively. After examining swirl peak locations and pressure gradients, the corresponding viscous core dimensions in the horizontal direction are found to be 12 and 17 mm. In conjunction with their counterparts from the vertical surveys and consistent with the flow visualizations of Refs. 13 and 20, primary vortices at the trailing edge are found to have an elliptical shape.

Distributions of Mach number component M_y, horizontally across the leading-edge vortices at the $z/c = 0.5$ plane are shown in Fig. 28. At this station, vortical trajectory is almost aligned with the probe direction and zero swirl locations coincide with the minimum pitot pressure point. Moreover, due to the absence of the wing surface, two distinct swirl peaks associated with each primary vortex emerge. Their inboard and outboard magnitudes for the 7-deg incidence angle are -0.78 and 0.86. The corresponding maximum M_y values for the 12-deg angle of attack are -1.22 and 1.43. It is evident

that these vortices are very strong, which is indicative of the lift generation capability associated with delta planforms in supersonic flight. The core dimension as determined from downstream horizontal surveys is 9 mm for both cases. These measurements reconfirm the vortex core shape adjustment with the downstream distance from the trailing edge during the near-wake vortex stretching, also noted in the vertical surveys. Traversing further toward the leading edge, one more vortical structure with the opposite rotation to that of the primary vortex is observed. This counter-rotating system is believed to be the secondary vortex, which, according to the low-speed findings of Hummel,[5] is known to orbit around the leading-edge vortex in the near wake before ultimately merging with it.

Figures 29–32 present the spanwise distributions of axial, M_z and total, M, Mach number in the near wake. In the trailing-edge plane, midspan values of the axial component are slightly higher than that of the freestream due to the acceleration of flow over the wing. As inferred from the preceding discussion on the M_y distribution, the core entrainment will draw on viscous fluid from the wing boundary layer and the shear layer originating from the leading edge. The resulting wakelike M_z and M profiles in the cores are again evident. At the trailing edge, the minimum axial Mach number in the core region of the 7-deg vortex is 1.58, as seen in Fig. 29, and the matching total Mach number of 1.87 is shown in Fig. 31. The corresponding values for the 12-deg case are $M_z = 1.59$ and $M = 1.97$. A higher incidence angle is seen to produce an increase in the spatial scale of the deficit region. Recall from the vertical surveys at the trailing edge that the lower portion of the vortex is bonded by a viscous structure. Similarly, the shear layer from the leading edge is believed to restrain the primary vortex from expanding in the spanwise direction, resulting again in the local Mach number rise. The axial Mach number deficits in the vicinity of the leading edge, illustrated in Fig. 29, closely coincide with the position of secondary vortices as revealed by the oil flow visualizations[14] and the accompanying pitot pressure deficits (Fig. 19). The wakelike profiles in both M_z and M are seen to persist into the half-chord survey plane. At the wake station $z/c = 0.5$, the axial Mach number in the core center for the 7-deg vortex is 2.28, as seen in Fig. 30, and the matching total Mach number of 2.34 is shown in Fig. 32. The corresponding values for the 12-deg case are $M_z = 1.69$ and $M = 1.78$. The total Mach number distributions in both measurement stations follow the general trend of the axial component contours, thereby once again confirming the dominance of the streamwise flow. The M_z and M distributions indicate that the convection of the vortex wake in the near field is complex and do not proceed as a uniform translation of the profiles found at the trailing edge.

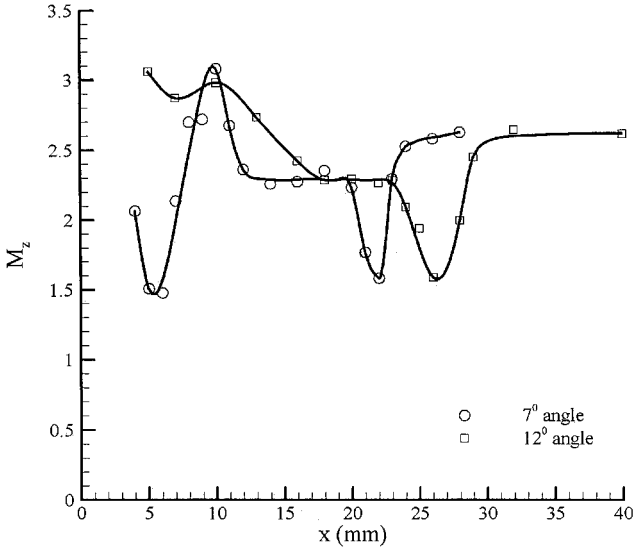

Fig. 29 Axial Mach number from the horizontal surveys at $z/c = 0$.

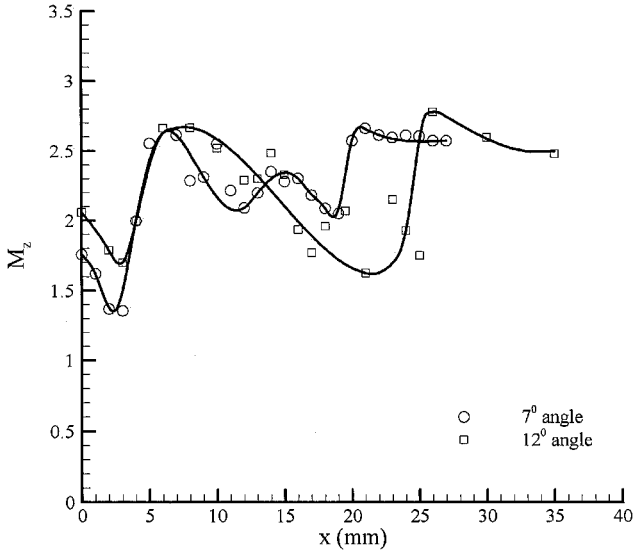

Fig. 30 Axial Mach number from the horizontal surveys at $z/c = 0.5$.

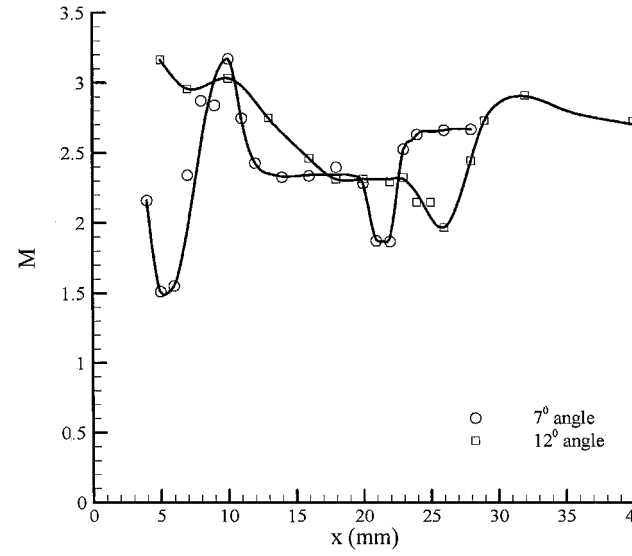

Fig. 31 Total Mach number from the horizontal surveys at $z/c = 0$.

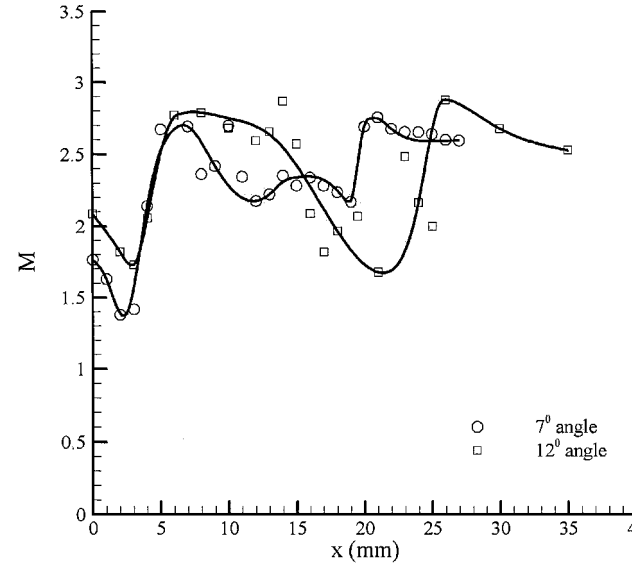

Fig. 32 Total Mach number from the horizontal surveys at $z/c = 0.5$.

Conclusions

An experimental study of a 75-deg sweptback, sharp-edged and flat-top delta wing near wake was done in a Mach 2.49 stream. Five-hole conical probe surveys were conducted vertically and horizontally through the primary vortices at the trailing edge and half a chord downstream of the planform for 7- and 12-deg angles of attack. These measurements were further complimented with shadowgraph visualizations of the flowfield. Spark shadowgraphs revealed information regarding the trajectory and relative size of the generated vortices while confirming that no probe-induced vortex breakdown had occurred. A novel approach of numerical calibration using a three-dimensional Navier–Stokes solver generated calibration data for the blunt-nose conical probe over a range of Mach numbers and pitch angles.

Pressure and Mach number distributions revealed a complex structure and convective character of the delta wing vortex wake. The primary vortex core at the trailing edge moved inboard and upward relative to the model surface as the incidence angle was increased. Registered downward motion of the vortex pair behind the wing is a consequence of a self-induction process as seen both in low- and high-speed studies. The magnitude of the pitot, total, and static pressure deficits increased with increasing angle of attack for the same measurement plane and reduced with the downstream distance from the model. Vertical traverses for the same survey station but a more elevated planform indicated growth in spatial scale of pressure deficits. Swirl Mach number profiles resemble a Lamb–Oseen vortex with a linear swirl distribution in the viscous core and velocity decay outside. Considerable swirl peaks with low supersonic and high transonic values are present in all vertical and horizontal surveys. An inward flow of substantial magnitude, directed toward the center at the core edges, is also found. The vortices, therefore, possess the ability to entrain surrounding fluid. The axial Mach number distribution in the investigated near field is wakelike, in agreement with the five-hole probe measurements in supersonic streams for the leading edge and tip vortices. Total Mach number profiles follow the general trend of axial component contours, confirming the prevalence of the streamwise flow. Consistent with the existing flow visualizations, measurements also illustrated vortex shape adjustment in the near wake. Primary vortices suppressed over the wing stretched downstream in the vertical direction.

The current study concurred with the existing notion that leading-edge vortices in supersonic flows have qualitative similarities to those at low speed. However, the investigation further demonstrated that quantitative differences do exist, particularly in the axial flow profiles. In the supersonic case, primary vortices are of significant strength, as seen by pressure and swirl magnitudes. They persist far downstream and, as such, the entertainment and mixing characteristics of the vortex wake can have important consequences to the injection of engine plumes issued in the wake. This has not only environmental implications in the case of fielding a future SST fleet, but also low observability considerations. For example, if utilized strategically, the strong vortices can provide rapid cooling needed to reduce signatures from engine exhausts. In light of the aforementioned representative practical applications, the current investigation is consistent with a number of aeronautical interests internationally and provides insights as to the nature of supersonic leading-edge vortices. In the process, the study further contributes to the scarce database available for calibrating computational fluid dynamics solvers.

Acknowledgments

Computing resources for this work were provided by Pittsburgh Supercomputing Center under Grant CTS930035P. The authors are grateful to Frank Marconi of Northrop–Grumman Corporation for the invaluable discussions pertaining the TLNS3D code, as well as for his encouragement. The authors would like to thank Anthony Castrogiovanni and Alexander Betti of GASL, Inc., for their assistance in the geometric characterization of the miniature probe. Finally, the advice and assistance with the flow visualization experiments provided by Frank Wang and the assistance of Lester Orlick during the experimental phase of the work is greatly appreciated.

References

[1]*Proceedings of the Conference on Atmospheric Effects of Aviation*, Virginia, May 1998.

[2]Seebass, R., and Charbonnier, J. M. (Ed.), "Fluid Dynamics Research on Supersonic Aircraft," RTO Educational Notes 4, NATO RTO-EN-4, Nov. 1998.

[3]Spreiter, J. R., and Sacks, A. H., "The Rolling up of the Trailing Vortex Sheet and Its Effect on the Downwash Behind Wings," *Journal of the Aeronautical Sciences*, Vol. 18, No. 1, 1951, pp. 21–32.

[4]Erickson, G. E., Peake, D. J., Del Frate, J., Skow, A. M., and Malcolm, G. N., "Water Facilities in Retrospect and Prospect—An Illuminating Tool for Vehicle Design," Aerodynamic and Related Hydrodynamic Studies Using Water Facilities, AGARD Conf. Proceedings, No. 413, 1987, pp. 1.1–1.27.

[5]Hummel, D., "On the Vortex Formation over a Slender Wing at Large Angles of Incidece," *High Angle of Attack Aerodynamics*, CP-247, AGARD, 1978, pp. 13-1–13-17.

[6]Hiremath, B. M., Holla, V. S., and Govindaraju, S. P., "Study of Flow Field in the Near Wake of Delta Wings," *Journal of Aeronautical Society of India*, Vol. 36, No. 1, 1984, pp. 17–27.

[7]Miller, G. D., and Williamson, H. K., "Turbulent Structures in the Trailing Vortex Wake of a Delta Wing," 1995.

[8]Perkins, E. W., and Canning, T. N., "Investigation of Downwash and Wake Characteristics at a Mach Number of 1.53, II–Triangular Wing," NACA RM A9D20, 1949.

[9]Boatright, W. B., "An Analysis of Pressure Studies and Experimental and Theoretical Downwash and Sidewash Behind Five Pointed-Tip Wings at Supersonic Speeds," NACA TR-1380, 1958.

[10]Centolanzi, F. J., "Measured and Theoretical Flow Fields Behind a Rectangular and a Triangular Wing up to High Angles of Attack at a Mach Number of 2.46," NASA TN D-92, 1959.

[11]Smith, L. G., Maurice, M. S., Seibert, G. L., and Tyler, C., "Laser Velocimetry Measurements of Supersonic Vortex Flows on a Simple Razor-Edged Delta Wing," AIAA Paper 91-1684, June 1991.

[12]Lang, N., "PIV Measurements in Sub- and Supersonic Flow over the Delta Wing Configuration ELAC," *Proceedings of the 8th International Symposium on Flow Visualization*, 1998, pp. 205.1–205.8.

[13]Ganzer, U., and Szodruch, J., "Vortex Formation over Delta, Double-Delta and Wave Rider Configurations at Supersonic Speeds," AGARD-CP-428, 1987, pp. 25-1–25-32.

[14]Milanovic, I. M., and Kalkhoran, I. M., "Numerical Calibration of a Conical Five-Hole Probe for Supersonic Measurements," *Measurements Science and Technology*, Vol. 11, No. 12, 2000, pp. 1812–1818.

[15]Vatsa, V. N., and Wedan, W. W., "Development of a Multigrid Code for 3-D Navier–Stokes Equations and Its Application to a Grid-Refinement Study," *Computers and Fluids*, Vol. 18, No. 4, 1990, pp. 391–403.

[16]Kalkhoran, I. M., Cresci, R. J., and Sforza, P. M., "Development of Polytechnic University's Supersonic Wind Tunnel Facility," AIAA Paper 93-0798, Jan. 1993.

[17]Smart, M. K., Kalkhoran, I. M., and Bentson J., "Measurements of Supersonic Wing Tip Vortices," *AIAA Journal*, Vol. 33, No. 10, 1995, pp. 1761–1768.

[18]Stromberg, A., Henze, A., Limberg, W., and Krause, E., "Investigation of Vortex Structures on Delta Wings," *Journal of Flight Sciences and Space Research*, Vol. 20, No. 2, 1996, pp. 71–79.

[19]Szodruch, J., "Lee Side Flow over Slender Delta Wings with Large Thickness-to-Chord Ratio," *ILR Bericht 23*, Techn. Univ. of Berlin, Berlin, 1977.

[20]Miller, D. S., and Wood, R. M., "Lee-Side Flow over Delta Wings at Supersonic Speeds," NASA Technical Paper 2430, 1985.